PERGAMON

Atmospheric Environment 34 (2000) 5319–5328

ATMOSPHERIC ENVIRONMENT

www.elsevier.com/locate/atmosenv

Reconstruction of the methane fluxes from the west Siberia gas fields by the 3D regional chemical transport model

S.V. Jagovkina[a,*], I.L. Karol[a], V.A. Zubov[a], V.E. Lagun[b], A.I. Reshetnikov[c], E.V. Rozanov[d]

[a]*Main Geophysical Observatory, St.-Petersburg, 194021, Russia*
[b]*Arctic and Antarctic Research Institute, St.-Petersburg, 199397, Russia*
[c]*Research Center for Atmospheric Remote Sensing, St.-Petersburg, 194021, Russia*
[d]*University of Illinois at Urbana-Champaign, 105 S. Gregory, Urbana, IL 61801, USA*

Received 30 January 2000; received in revised form 16 May 2000; accepted 7 July 2000

Abstract

A 3D mesoscale tropospheric photochemical transport model of high spatial resolution has been developed and used for assessment of the methane concentrations and methane emission in the West Siberian region of intensive mining of natural gas and oil deposits. The model is validated against the measurements of methane concentration at the surface and in the lower troposphere collected during July 1993 and June 1996 experiments. Comparison of the simulated and observed concentrations allowed to estimate that during the above periods the average natural methane fluxes were as high as $65\,mg\,m^{-2}\,day^{-1}$. The anthropogenic methane fluxes (leakage from gas deposits) integrated over model domain during the same time period were about 20% of the total methane emission from relevant areas.

Keywords: Anthropogenic and natural source emission; Model estimations

1. Introduction

The estimation of methane emission intensity is among the most important and difficult in the greenhouse gas (GG) global emission inventories problem, because the numerous natural and anthropogenic methane sources have rather high variability in space and time (Khalil, 1993). The northwest Siberian (NWS) region takes an exceptional place among other territories due to the presence of large methane sources there. These sources are of natural (wetlands, tundra ecosystems, permafrost areas) as well as man-made (gas leakage from the big system of gas wells, gas and oil transport pipelines) origin. Both sources make a significant input into the global CH_4 releases into the atmosphere (Andronova and Karol, 1993; Matthews, 1993; Beck et al., 1993; Bartlett and Harriss, 1993; Hein et al., 1997, Reshetnikov et al., 2000).

The intensity of the most of NWS methane sources has been estimated indirectly on the basis of the published gas mining volume and leakage percent from wells and pipes (e.g., Andronova and Karol, 1993; Beck et al., 1993; Reshetnikov et al., 2000) or by extrapolating of measured CH_4 natural flux values from the North American wetlands to the NWS ones (see the review by Bartlett and Harriss (1993) as an example). These estimations vary in a wide range (see Table 1) and are highly uncertain. Few direct measurements of CH_4 fluxes from NWS areas such as Vasuygan wetlands (Panikov et al., 1995) and a tundra on the shore of Arctic Ocean (Christensen et al., 1995), demonstrated extremely high spatial and temporal variability of the sources.

The methane fluxes have also been estimated from the solution of inverse problems for the global models of transport and photochemistry (Brown, 1993, 1995; Hein

* Corresponding author. Tel./fax: +7-812-247-86-68.
E-mail address: svetlana@main.mgo.rssi.ru (S.V. Jagovkina).

1352-2310/00/$ - see front matter
PII: S1352-2310(00)00347-2

Table 1
Estimates of methane emissions from some sources in CIS, West Siberia, Canada and Alaska[a]

Source	Region	Area (10^{10} m^2)	CH_4 flux (mg m^{-2} day^{-1})	Total annual Mt CH_4 yr^{-1}	Comment	Reference
Wet tundra	Alaska	33	100 (3–360)	5.9	July–August	Bartlett and Harriss (1993), Matthews (1993)
Dry tundra	Alaska	33	10 (1–30)	5.9	July–August	Bartlett and Harriss (1993), Matthews (1993)
Forested fen	Canada	127	24 (0–1800)	11	June–August	Bartlett and Harriss (1993), Matthews (1993)
Unforested fen	Canada	127	30 (0–110)	11	June–August	Bartlett and Harriss (1993), Matthews (1993)
Flooded pools	Canada	—	30–50 (10–60)	—	June–September	Bartlett and Harriss (1993)
Lakes	Canada	—	170 (12–520)	—	Summer	Bartlett and Harriss (1993)
Wetlands	NWS	45	6.3	1.1	Indirect estimations	Andronova and Karol (1993)
Wetlands	NWS	150	65	10	Extrapolation from July data	This work
Palsa bog (dry tundra)	Yamal sea shore	—	1.4 (0.4–5) 0.05 (0–5)	—	Measured in August	Christensen et al. (1995)
Wet tundra	Yamal sea shore	—	105 (54–170) 9.8 (0–39)	—	Measured in August	
Boreal forest	Canada 53.5°N	— —	27 (2–37)	—	In July, August; two weeks mean	Simpson et al. (1997)
Gas wells	NWS	1.8	1500	~ 10	Estimated in 1994	Bosnyatskiy and Shilov, 1994
Gas wells	NWS	—	—	8.5	Estimated for 1988	Andronova and Karol (1993)

[a]Estimated by extrapolation of summer months data to the whole year. Upper bound of the real value.

et al., 1997), but without fair estimation of the regional source distributions and intensities.

This study presents one of the first attempt of such an evaluation by using the specially designed mesoscale 3D Chemical Transport Model (CTM) which includes the real wind field in the troposphere (above 1 km) over the modeled area and calculated planetary boundary layer (PBL) winds. The model input parameters (such as surface methane fluxes from natural sources) were adjusted to match the available CH_4 observation data collected in the NWS area, namely the aircraft measurements in July 1993 (Tohjima et al., 1997) and measurements in the ground surface air at one point of the southeast part of Yamal Peninsula in June 1996 (Reshetnikov et al., 1996). The computational efficiency of the model allowed to carry out a large number of numerical experiments, following the wind fields and temperature data changing from day to day in the PBL and in the free atmosphere over the modeled region. The obtained from the model simulations CH_4 ground surface source intensities are estimated and discussed.

2. Description of the model

A 3D Tropospheric Chemical Transport Mesoscale Model (MGO 3D-TCTMM) has been developed and applied for simulations of tropospheric methane distribution over the West Siberian region. The model domain is 58–73°N and 62–82°E (62–110°E – in extended version). The spatial grid has 0.5° latitude and 1.0° longitude resolution. The log-pressure coordinate system is utilized in the vertical direction with 10 unevenly spaced levels from the ground up to approximately 1 km (5, 10, 40, 80, 120, 250, 400, 600 and 800 m) and 10 levels from 1 up to 11 km with the 1 km resolution. Time step $\Delta t = 15$ min is used for the model integration. The model version with fixed dynamical parameters usually takes 4–5 model days to reach steady-state regime. Most of the calculations ran for 1–3 model months with dynamical parameters updated and recalculated every day.

2.1. Parameterization of planetary boundary layer

The vertical profiles of turbulent coefficient K_{zz}, horizontal wind components, temperature (T) and the thickness of quasi-stationary planetary boundary layer were derived from the wind, temperature and geopotential height data at the 850 hPa levels and from the observed ground temperature fields. The stratification parameter μ inside of the PBL has been calculated according to the parameterization of Penenko and Aloyan (1985). This parameter is used to correlate the synoptic data with the internal PBL parameters. Then, the approach developed by Zilitinkevich (1970) and Bobyleva (1970) for vertical profiles of wind and K_{zz} was applied. These parameterizations specify all parameters as calculated functions of Rossby number, $Ro = V_G\ (f \cdot z_o)^{-1}$ (where V_G is the absolute value of geostrophical wind velocity at the PBL upper boundary, f is the Coriolis parameter and z_o is the roughness length) and of the PBL external stratification parameter $S = (\kappa^2 \beta\, \delta\Theta)(fV_G)^{-1}$ where κ is the von Kármán constant, β is the buoyancy parameter and $\delta\Theta$ is the integral vertical potential temperature difference across the PBL. The parameterization ends up with the relationships for zonal (U) and meridional (V) wind components in the following form: $U(z) = V_G \cos\alpha + \varphi(\mu, z)$, $V(z) = V_G \sin\alpha - \psi(\mu, z)$ and $K_{zz} = \zeta(\mu, z)$, where $\varphi(\mu, z)$, $\psi(\mu, z)$, $\zeta(\mu, z)$ and the angle of full wind rotation inside the PBL $\alpha = A(S, Ro)$ are the automodeled solution of the equation set for PBL (Bobyleva, 1970). Such parameterization of PBL allows to exclude the influence of the surface small-scale roughness on the calculated values by using the external parameters.

2.2. Transport parameters in the free atmosphere

Between the top of the PBL and 1 km level, the wind is considered as a geostrophical and is defined by the wind velocity at the 850 hPa surface. The vertical turbulent coefficient K_{zz} between the top level of PBL and 1 km is assumed to be 10% of its PBL maximum (Lee and Larsen, 1997). The value of K_{zz} was set equal to 10 m^2 s^{-1} above 1 km level (Prather and Remsberg, 1993). For the free atmosphere up to 100 hPa level as well as for 850 hPa level the observed horizontal winds and temperature data from the Russian ground stations located in the considered and adjacent areas of the northern West Siberia were used.

2.3. The development of the meteorological fields database

The data have been extracted from the Russian meteorological data set for the concerned region for July of 1993 and for June of 1996 (for 12 GMT) and then converted by the objective analysis method onto the model regular grid according to the scheme proposed by Lagun et al. (1980). The spatial interpolation procedure of the meteorological parameter fields consisted of two steps:

(1) The coarse grid data set was created from the observed data at the irregular net of meteorological and aerological stations by splitting of the considered region into triangles using the finite element method (Zienkiewicz, 1971). This data grid had the resolution of 300–500 km that is comparable with the distances between points of the measurements located in the considered area. At the same time this grid resolution corresponded to the scales of the tropospheric synoptic disturbances prevailed in considered region (such as cyclones, anticyclones, edges and troughs) which are responsible for the air mass transport. Therefore,

such data grid allowed to describe the internal structure of the synoptic events with horizontal scales of about 1500–2000 km;

(2) for the preparation of the final 3D data set with spatial resolution 40×50 km the spline interpolation technique (Ahlberg et al., 1967) of the meteorological fields was utilized. This method provided a smoothness of the analyzed fields, but it did not mask their subsynoptic features. A comparison of the interpolated meteorological fields over the model region with the NCEP/NCAR Reanalysis data (Kalnay et al., 1996) at the $2.5^\circ \times 2.5^\circ$ latitude–longitude grid showed their fair qualitative agreement for large-scale atmosphere circulation features, but the objective analysis scheme used here provided more detailed mesoscale pattern representation.

2.4. Numerical scheme for gas transport

The second moment conservation scheme (Prather, 1986) was used for the description of the advective transport of species. Vertical diffusion was calculated by the implicit centered space differences scheme (Fletcher, 1998). The effect of horizontal diffusion is considered to be negligible in comparison with the advective horizontal transport by winds.

2.5. Chemistry

The photochemical scheme included 21 gas species, of O-, N-, H-, C-groups and products of methane oxidation. Kinetic rates of about 71 gas-phase reactions were taken from JPL-97 (DeMore et al., 1997). Fully implicit iterative Newton–Raphson numerical scheme was used for the calculation of the gas mixing ratio. This scheme possesses first-order accuracy in time, it is very computationally stable and does not produce negative concentrations. The applied chemistry routine is similar to the method described by Rozanov et al. (1999).

2.6. Boundary conditions

The methane mixing ratio was prescribed at the model domain side "walls" when the wind was directed into the region. In the opposite case the absence of the species horizontal gradient was assumed at the "walls". The prescribed methane mixing ratio was set equal to 1.95 ppmv in the lower 1 km at the southern "wall" (Bergamaschi et al., 1998) and 1.8 ppmv in the area above 1 km and at all other "walls" including the upper boundary according to the estimation published by Tohjima et al. (1997). Prescribed methane fluxes at the ground surface were adopted as a lower boundary condition. For the natural methane source intensities in each lower box of the model area the first assumption was made on the basis of the geographical distribution of the marshes (Melnikov and Moskalenko, 1991) and of their surface temperature regime for summer months (some information about the temperature dependence of methane fluxes was taken from Whalen and Reeburgh (1988); Sebacher et al. (1986)). For the tundra and wetlands methane fluxes the initial range was chosen within 2–150 mg $CH_4\ m^{-2}\ day^{-1}$ depending on the prevailed type of underlying surface in the model box (Matthews and Fung, 1987; Matthews, 1993; Andronova and Karol, 1993; Bartlett and Harriss, 1993; Christensen et al., 1995). The location of the gas fields and their relative gas leakage intensities were prescribed on the basis of summarizing map of gas and oil deposits in the North of Tumen area, (VNIIGAZ, 1998 Gaspron Moscow). Then the values of leakage were normalized in agreement with the estimations of Bosnyatskiy and Shilov (1994) and were prescribed as 1–2 g $CH_4\ m^{-2}\ day^{-1}$. The spatial distribution of methane fluxes adopted in model is presented in Fig. 1. The actual methane emissions from the modeled region were estimated by comparison (and subsequent adjustment of the source intensity) of the simulated methane mixing ratio vertical profiles with the measured ones in several points of the region.

3. Results for July 1993 period

The developed model was tuned and validated against available observations. The model ran for 1–3 months from the uniform initial distribution of methane mixing ratio (1.8 ppmv) and with the boundary conditions described above. The natural methane fluxes were adjusted to obtain the best agreement between simulated and observed (Tohjima et al., 1997; Nakazawa et al., 1997) vertical profiles of CH_4. These data were collected during

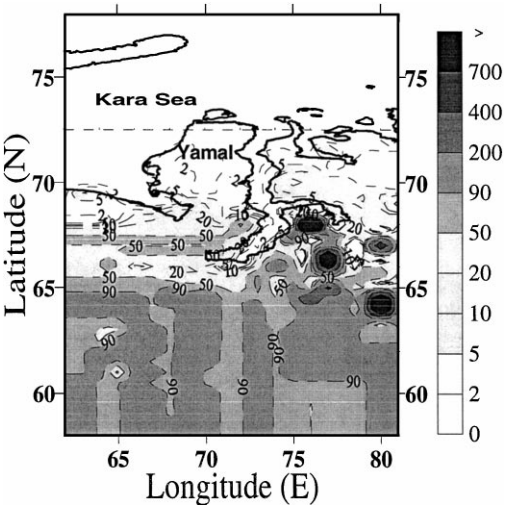

Fig. 1. Total surface methane fluxes (mg $m^{-2}\ day^{-1}$) adopted in the model for June/July.

the airborne measurements of methane concentrations performed over the West Siberian region in July 1993. The data consist of the vertical profiles when the aircraft flew at different altitudes from 80 m up to 1–2 km level, and horizontal cross sections of methane mixing ratio for the same levels for few points inside the considered region. Both the data sets were used for adjusting of the surface methane fluxes intensities. All points of the measurements were located far enough from the considered gas deposition fields (in the southern part of the region with marshes emitting a lot of methane in the summer period, as well as over the northern tundra with small natural methane fluxes) and the sensitivity of the model methane concentrations to the variations of anthropogenic fluxes was negligible for these experiments. The sensitivity of the model results to the prescribed natural methane fluxes depended on the location and date of the measurements, i.e. on the specific meteorological situation. In this set of calculations, the area near Khanty–Mansiysk on 23–24 July was found to be the most sensitive. Except for the natural methane fluxes intensities, we varied the most uncertain parameters of the model such as (1) the coefficient of vertical turbulent diffusion, which is calculated inside the PBL module and can be defined only theoretically, and (2) the methane concentration for the south boundary condition, which was set on the basis of measurements in summer conditions (e.g., Bergamaschi et al., 1998), but exceeds the usual background methane mixing ratios. The results of the sensitivity tests are presented in Table 2.

Table 2 demonstrates that the simulated methane concentrations are the most sensitive to the changing of natural methane fluxes in the areas under consideration. Even in the less sensitive place (Tazovskiy region) the imposed 50% variation of the natural methane flux caused the most prominent (among three tests) variations of methane concentrations. On the basis of the model experiments with different intensities of surface methane fluxes we defined the natural methane fluxes as $160 \pm 40\,mg\,m^{-2}\,day^{-1}$ for Khanty–Mansiysk region, $120 \pm 50\,mg\,m^{-2}\,day^{-1}$ for Nizhnevartovsk area, and as $20 \pm 7\,mg\,m^{-2}\,day^{-1}$ for tundra near Tazovskiy. The measured and simulated methane vertical profiles are presented in Fig. 2. The error bars of measured values indicate the spatial variability of the measurement data over the horizontal path of aircraft. Both profiles are in a rather good agreement in the layer of almost constant methane mixing ratio above the PBL. Slightly worse agreement of calculated and measured methane concentrations was found in the PBL and just over it, which reflects the high local variability of simulated and observed methane distribution in space and time. Such a disagreement could be explained by using diurnally averaged PBL in the model. It should be noted, however, that the measurements were carried out in various daytime hours, predominately in the morning when the boundary layer is not yet well formed. As has been pointed out by Worthy et al. (1998), the continuous methane measurements in the ground surface air in boreal site (Ontario, Canada) revealed substantial diurnal variations in July and August with maximum in the morning (see also Fig. 2).

Some example of the calculated latitude–longitude cross-sections of the methane mixing ratios predominantly at 100 m height for 23 July 1993 is depicted in Figs. 3(a) and (b) together with the aircraft measurement data. The location of the measurement area (white rectangles) and the measured methane mixing ratios are indicated in the figures. A good agreement of the measured and calculated values is partly the result of the above mentioned methane surface flux adjustment to the measured profiles. It is also evident, that the using of

Table 2
The response of calculated methane concentrations to variation of input model parameters

Test	Nizhnevartovsk (21 July 1993) 61.5°N, 79°E	Khanty–Mansyisk (23 July) 61°N, 69.5°E	Khanty–Mansyisk (24 July) 61°N, 69.5°E	Tazovskoe (27 July) 67.5°N, 79°E
Variation of K_{zz} inside PBL				
50% reduction	< 1%	4%	4%	< 0.1%
300% increase	< 1%	6%	6%	< 0.2%
Variation of the south boundary condition				
1.8 ppm	3%	2.5%	2%	0.5%
2.0 ppm	2%	1%	0.5%	0.2%
Variation of the natural fluxes over the whole model area				
± 50%	± 3.5%	± 9%	± 14%	± 0.7%
100% increase	7%	18%	28%	1.5%

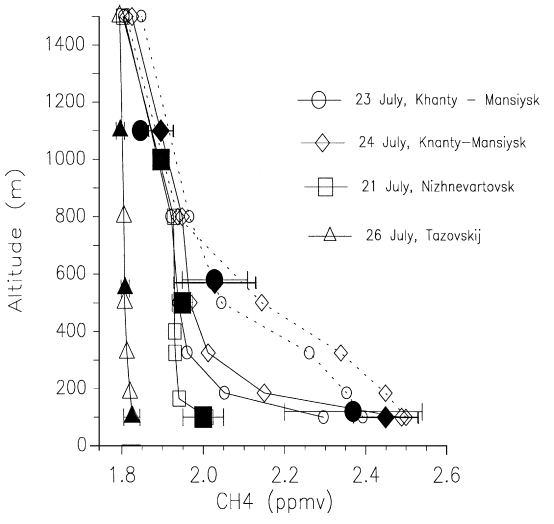

Fig. 2. Vertical profiles of methane mixing ratio (ppmv) simulated and measured on July, 1993. Open marks indicate model results, solid marks indicate measurements (data from Tohjima et al., 1997), the error bars for measurement values present the averaging over the flight path, its length is comparable with the model horizontal box sizes. Dashed lines present the model results for first part of day, solid lines are the calculations at the end of day.

the real wind field, even measured once a day, critically determines methane concentration fields over the emission region at rather large scales with significant day to day variability of these fields due to the wind variations.

On 28 July, the aircraft crossed and registered the methane mixing ratio maximum during the flight from Nizhnevartovsk to Yakutsk in the AM hours (Tohjima et al., 1997). An attempt to trace the similar "cloud" advection at the 7 km level during 28 July to the east of gas well areas has been performed with our model and the result is presented in Fig. 4 which shows that the calculated methane mixing ratios are also very close to the measurements. For the model experiment with exclusion of all gas wells sources in the region (the numbers in brackets) the methane mixing ratios at the 7 km and about 800 km to the NE from these sources differed from the results of calculations with account of the anthropogenic origins in less than 1% and this value is within the model accuracy. This example showed that the estimation of the gas well and transport pipe methane emissions by such distant aircraft measurements in NWS is impossible at least in the summer when all natural methane sources are active. Probably, it can be done on the basis of winter time measurements when the natural methane sources are isolated by the frost, snow and ice cover. However, some snap-shot estimations of the methane fluxes from the underlying surfaces in the areas of flight measurements are possible.

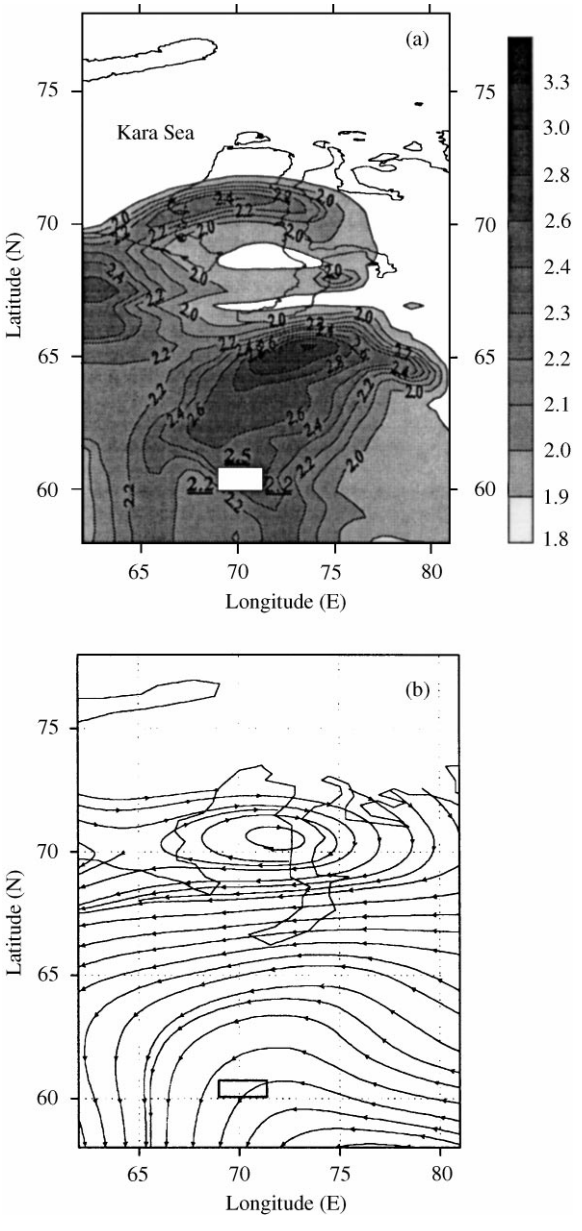

Fig. 3. (a) Measured (underlined numbers) and simulated CH_4 mixing ratio (ppmv) at $h \sim 100$ m on 23 July 1993 over Khanty–Mansiysk. (b) The stream function of wind for $h \sim 100$ m on 23 July 1993. The white square indicates the area of measurement near Khanty–Mansiysk.

4. Results of the 1996 summer simulations and comparison with the observed data

The MGO 3D-TCTM model was also used to evaluate the surface methane distribution for June 1996 and to compare the appropriate model data with the methane

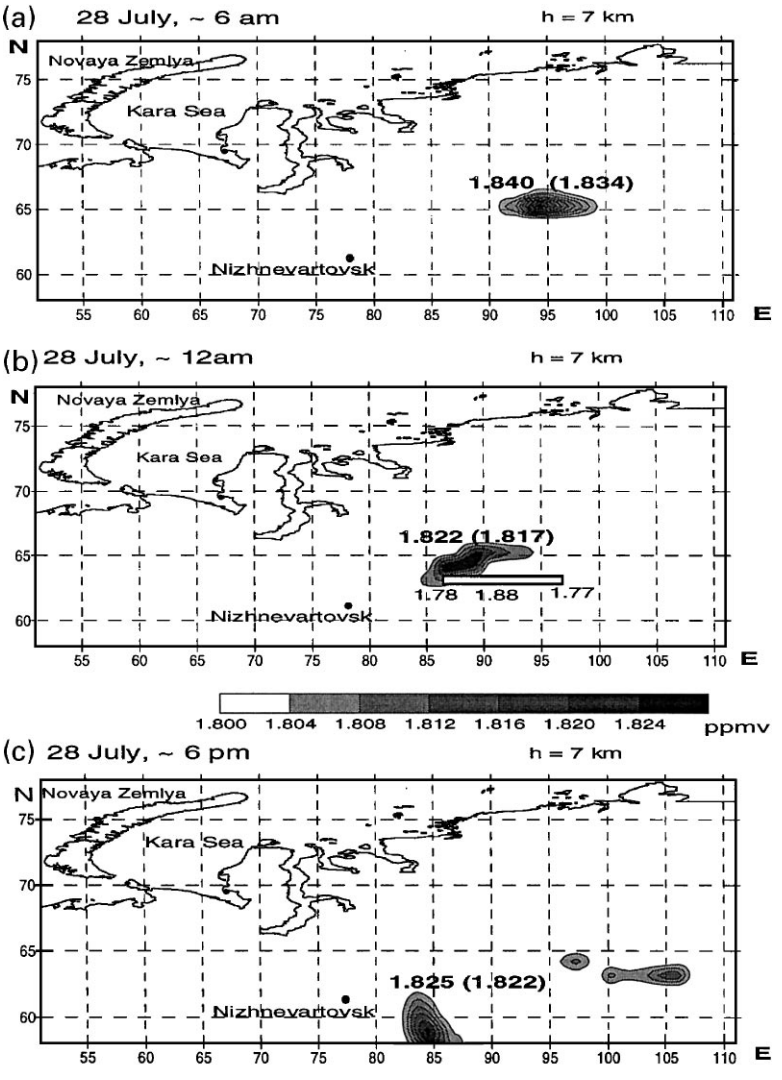

Fig. 4. Methane mixing ratio (ppmv) at $h = 7$ km calculated for 28 July 1993 and measured (grey bar at b) around midday to the east of Nizhnevartovsk (numbers in brackets show CH_4 mixing ratio, calculated with natural source only).

mixing ratios obtained during the measurement campaign (Reshetnikov et al., 1996). Then, the preliminary estimation of methane surface source intensity in the region of gas deposits was made.

The measurements were carried out in one point located in the southern part of Yamal Peninsula at the 250–500 km distance from the gas deposits fields. The data sampling was performed in flasks at daytime during few days from 12 to 24 June 1996. The wind speed and wind direction at the level of 2 m above the surface were also registered at the sampling moment. More detailed description of the experiment was presented by Reshetnikov et al. (1996).

In these calculations, we applied the same natural methane surface fluxes as for July 1993. Fig. 5 presents the measured methane concentrations versus calculated ones. The daily averaged PBL winds used for calculations during the indicated time period in the sampling point and measured winds at the 2 m level are presented in Table 3. The measured wind with 110–190° azimuth from the North was directed from the gas fields area. The directions of the calculated and measured winds were opposing each other on 13 and 14 June. Some discrepancy can be also seen for few other days. The disagreement of the calculated and measured wind directions can be explained by the differences in the diurnally averaged winds adopted in the model and measured once or twice a day ground surface wind directions and velocities (as an example on 13 June, the measured wind rotated about 170° during 8 h which cannot be matched by the model).

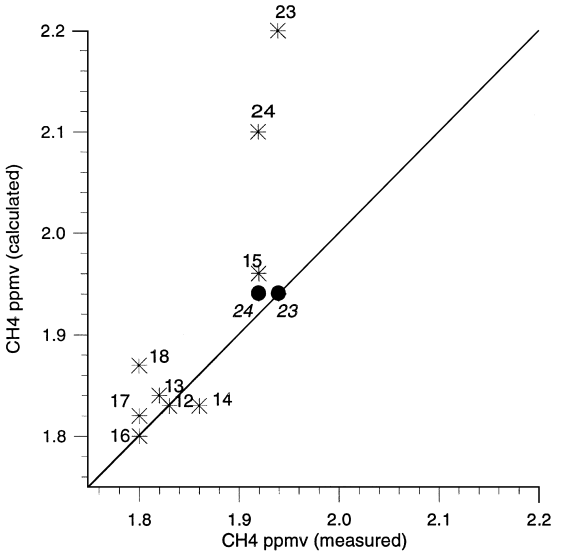

Fig. 5. Measured and simulated CH_4 concentrations for Yamal experiment on 12–24 June 1996. Numbers above the data points are the dates. Crosses indicate the calculation results for the gas leakage source intensity of $10\,Mt\,CH_4\,yr^{-1}$ and for $1–2\,mg\,m^{-2}\,day^{-1}$ intensity of the natural fluxes in tundra, circles indicate the calculation results for $7\,Mt\,CH_4\,yr^{-1}$ deposits leakage intensity and for the same intensity of natural fluxes in tundra. Except for two days (23 and 24 June) the model results for both scenarios almost coincide.

Table 3
The measured and modeled wind speed and wind direction in the sampling point

Date	Local time	Measured wind		Modeled wind	
		$m\,s^{-1}$	Azimuth	$m\,s^{-1}$	Azimuth
12	12:40	3	325	2.2	290
13[a]	11:11	2.5	190	2.2	293
13	19:50	1	20	2.2	293
14[a]	7:30	3	170	2.2	290
15	6:00	4	210	1.2	256
16	6:15	6	320	5.8	355
17	14:20	2	40	2.5	28
18	9:11	3	80	2.4	84
19[a]	9:40	3	110	1.0	114
19[a]	18:05	6	100	1.0	114
20[a]	6:03	7	100	1.4	153
20[a]	13:25	5.5	100	1.4	153
23[a]	15:58	4	170	3.7	150
24[a]	6:02	5.5	130	3.6	182

[a]Measurements accompanied by the wind blowing from the sector with gas deposits.

However, the both calculated and measured winds from the free of strong methane sources sectors were accompanied by low methane concentrations (on 12, 13, 16 and 17 June). On the basis of the best agreement of measured and modeled methane concentrations for these days the natural methane fluxes for tundra for this period (the beginning of the summer) were estimated as $1–2\,mg\,m^{-2}\,day^{-1}$. The wind from the sector of gas deposits (on 19, 20, 23 and 24 June) was accompanied by the maximal methane concentrations at the sampling point. The modeled wind speed agrees with the measurements rather good except of 19 and 20 June. For these two days the modeled wind velocity appears to be much smaller than the measured wind and, as a consequence, the simulated methane concentrations are much greater than measured ones. Therefore, we did not consider these two days for estimations. There is about 10% difference in the measured (as well as calculated) methane mixing ratios between the days with the wind from the gas fields (23 and 24 June) and days when other wind directions prevailed. The simulated methane concentration sensitivity to the threefold vertical diffusion coefficient variations is within 3 and 5% depending on the day.

The error due to averaging over the model box does not exceed 2% for 12–18 June (when the methane horizontal distribution was rather smooth) and is about 5% for 23 and 24 June. Therefore, the obtained difference about 10% can be qualified as significant in comparison with the model accuracy and allows to conclude, that the anthropogenic source intensity (Q_f) averaged over the gas fields region was close to the value of $10\,Mt\,CH_4\,yr^{-1}$ adopted in the model from the data of Bosnyatskiy and Shilov (1994) for main Siberian gas deposits leakage. Few numerical experiments with the different intensity of deposits source ($\pm$ 50% of Q_f) demonstrated that the initial value of $10\,Mt\,CH_4\,yr^{-1}$ is the upper estimation for this area of gas deposits and for the particular year, and the value of $7\,Mt\,CH_4\,yr^{-1}$ agreed with the results of numerical experiments better (see Fig. 5). This estimation does not include the leakage from gas pipelines, which demands separate consideration and that be comparable with the leakage from gas deposits (Reshetnikov et al., 2000). For these numerical experiments, the seasonal homogeneity of the gas deposits leakage was suggested.

The above-described model calculations allowed us to estimate the intensities of natural and anthropogenic surface methane fluxes (leakage from main gas deposits). The appropriate surface areas are the following: the modeled area S_n is $1.52\times10^{12}\,m^2$ (for 58–73°N × 62–81°E), the gas well fields area S_f is $5\times10^{10}\,m^2$ ($S_f/S_n = 3.2\%$). The corresponding CH_4 total flux Q_n is $1.0\times10^{11}\,g\,CH_4\,day^{-1}$ from wetlands and tundra (for July) and Q_f is $(1.92–2.74)\times10^{10}\,g\,CH_4\,day^{-1}$ from the gas/oil wells (estimations were made on the basis of data published by Reshetnikov et al. (2000) and these model calculations). Therefore, the natural methane flux averaged over the whole area is $F_{av} = Q_n/S_n \cong 65\,mg\,m^{-2}\,day^{-1}$ and share the anthropogenic source of methane in the considered region in July

1993 (June 1996) was $Q_f/(Q_f + Q_n) \approx 20\%$ of total methane source intensity. Thus, the continuous monitoring of CH_4 emissions is desirable not only for gas wells and transport pipes but also for the wetland areas.

Table 1 gives the published estimations of methane emissions from the NWS region and the integrated CH_4 flux for July in the considered area from wetlands and gas wells adopted in the model. Analysis of the Table 1 reveals that the model estimate of natural methane flux from the considered region fits well to the range of measured methane fluxes in tundra, forested and unforested fens of Alaska and Canadian midland.

5. Discussion and conclusions

The presented comparison of the measured and modeled methane mixing ratios demonstrates that the developed mesoscale tropospheric transport model with assimilated wind data matches fairy well with the observed methane concentrations in the ground air and in the free troposphere over the NWS in the summer of 1993 and 1996. The comparison of the measured and simulated methane vertical profiles allowed to estimate the intensity of the methane emissions from the considered area for midsummer. These emissions fit well into the range of observed methane fluxes from various tundra and wetland places in Alaska and central Canada (Table 1).

During summer, rather intensive methane emissions from various wetland types are considerably masking the emissions from gas/oil mining and transporting pipelines in the concerned region. Preliminary estimates showed that the contribution of anthropogenic source does not exceed 20% of the total methane emission from the NWS region in the summer and the upper limit of the former is estimated as $10\,\mathrm{Mt\,CH_4\,yr^{-1}}$. Better conditions for monitoring of the gas/oil mining emissions could be found in winter/spring season, when the methane natural sources are locked or at least seriously reduced by the ice and snow cover.

The analysis of the calculated methane concentrations as well as the airborne and ground based measurements of methane in separate points (especially in the points located rather far from the wells) showed that the remote measurements are practically useless for the evaluations of the deposits source intensity. Therefore, for the methane emission monitoring from natural and anthropogenic sources, the problem of optimal placement of methane measurement points becomes very actual.

Acknowledgements

This study was supported by Russian Fund for Basic Research and INTAS (Grant INTAS-RFBR-95-0696, Grant INTAS 97-2055, and partly Grant 97-05-64266; 00-05-64254). We thank the anonymous reviewers for their kind and valuable comments.

References

Ahlberg, J.H., Nilson, E. N., Walsh, J. L., 1967. The Theory of Splines and Their Applications. Academic Press, New York and London, 298pp.

Andronova, N.G., Karol, I.L., 1993. The contribution of USSR sources to global methane emission. Chemosphere 26 (1–4), 111–126.

Bartlett, K.B., Harriss, R.C., 1993. Review and assessment of methane emissions from wetlands. Chemosphere 26, 261–320.

Beck, L.L., Piccot, S.D., Kirchgessner, D.A., 1993. Industrial sources. In: Khalil, M.A.K. (Ed.), Atmospheric Methane: Sources, Sinks and Role in Global Change. NATO ASI Series I, Vol. 13. Springer, Berlin, pp. 399–431.

Bergamaschi, P., Brenninkmeijer, C.A.M., Hahn, M., Rockmann, T., Scharffe, D.H., Crutzen, P.J., Elansky, N.F., Belikov, I.B., Trivett, N.B.A., Worthy, D.E.J., 1998. Isotope analysis based source identification for atmospheric CH and CO sampled across Russia using the Trans-Siberian railroad. Journal of Geophysical Research 103, 8227–8235.

Bobyleva, I.M., 1970. Calculation of turbulent characteristics in atmospheric planetary boundary layer, Trudy LGMI. Gidrometeoizdat 40, 3–63 (in Russian).

Bosnyatskiy, G.P., Shilov, Y.S., 1994. Technogenic processes, greenhouse effect and climate. Gazov. Prom. 3, 25–27 (in Russian).

Brown, M.K.M., 1993. Deduction of emissions of sources gases using an objective inversion algorithm and a chemical transport model. Journal of Geophysical Research 98, 12639–12660.

Brown, M.K.M., 1995. The singular value decomposition method applied to the deduction of the emissions and the isotopic composition of atmospheric methane. Journal of Geophysical Research 100, 11425–11446.

Christensen, T.R., Jonasson, S., Callaghan, T.V., Havstrom, M., 1995. Spatial variation in high-latitude methane flux along a transect across Siberian and European tundra environments. Journal of Geophysical Research 100 (D10), 21035–21045.

DeMore, W.B., Sander, S.P., Hampson, R.F., Kurilo, M.J., Golden, D.M., Horward, C.J., Ravishankara, A.R., Molina, M.J., 1997. Chemical Kinetics and Photochemical Data for use in Stratospheric Modeling, Evaluation 12. J.P.L. Publ., Pasadena, California, 256pp.

Fletcher, C.A.J., 1988. Computational Techniques for Fluid Dynamics, Vol. 1. Springer, Berlin.

Hein, R., Crutzen, P.J., Heimann, M., 1997. An inverse modeling approach to investigate the global atmospheric methane cycle. Global Biogeochemical Cycles II (1), 43–76.

Kalnay, E., et al., 1996. The NCEP/NCAR 40-year reanalysis project. Bulletin of the American Meteorological Society 77 (3), 221–248.

Khalil, M.A.K. (Ed.), 1993. Atmospheric Methane: Sources, Sinks, and Role in Global Change. NATO ASI Series I, Vol. 13. Springer, Berlin, 561pp.

Lagun, V.E., Romanov, V.F., Safronov, V.A., Smirnov, N.P., 1980. A method for interpolation of field experiment data. Meteorology and Hydrology 12, 48–53 (in Russian).

Lee, H.N., Larsen, R.J., 1997. Vertical diffusion in the lower atmosphere using aircraft measurements of ^{222}Rn. Journal of Applied Meteorology 36, 1262–1270.

Matthews, E., Fung, I., 1987. Methane emission from natural wetlands: global distribution, area, and environmental characteristics of sources. Global Biochemical Cycles 1 (1), 61–86.

Matthews, E., 1993. Wetlands. In: Khalil, M.A.K. (Ed.), Atmospheric Methane: Sources, Sinks and Role in Global Change NATO ASI Series, Vol. 13. Springer, Berlin, pp. 314–361.

Melnikov, E.S., Moskalenko, N.G. (Eds.), 1991. Map of Natural Complexes of the Northern West Siberia, WSEGINGEO (in Russian). Hydrogeology and Engineering Geology Research Institute, Moscow.

Nakazawa, T., Sugawara, S., Inoue, G., Machida, T., Makshyutov, S., Mukai, H., 1997. Aircraft measurements of the concentrations of CO_2, CH_4, N_2O and CO and the carbon and oxygen isotopic ratios of CO_2 in the troposphere over Russia. Journal of Geophysical Research 102 (D3), 3843–3860.

Panikov, N.S., Sizova, M.V., Zelenev, V.V., Mohov, G.A., Naumov, A.V., Gadzhiev, I.M., 1995. CH_4 and CO_2 emission from some Vasuygen wetlands: spatial and temporal variation of fluxes. Ecol. Chemistry 4, 13–23.

Penenko, V.V., Aloyan, A.E., 1985. Models and Methods for Problems of Environment Protection. Nauka, Novosibirsk 256pp (in Russian).

Prather, M., 1986. Numerical advection by conservation of second-order moments. Journal of Geophysical Research 91 (D6), 6671–6681.

Prather, M., Remsberg, E. (Eds.), 1993. The atmospheric effects of stratospheric aircraft. Report of the 1992 Models and Measurements Workshop, Vol. I. NASA Reference Publication, 1292, Washington D.C., 352pp.

Reshetnikov, A.I., Zinchenko, A.V., Paramonova, N.N., Privalov, V.I., Smetanin, G.C., Jakovlev, O.N., 1996. Preliminary estimations of methane emissions in the atmosphere from the biggest exploited gas wells of Western Siberia. Proceedings of the Conference on Environmental Protection by Prospecting and Exploitation of Hydrocarbon Fuels, Their Processing And Transportation, VNIGRI, St. Petersburg, pp. 78–80 (in Russian).

Reshetnikov, A.I., Paramonova, N.N., Shashkov, A.A., 2000. An evaluation of historical methane emissions from the Soviet gas industry. Journal of Geophysical Research 105 (D3), 3517–3529.

Rozanov, E.V., Zubov, V.A., Schlesinger, M.E., Yang, F., Andronova, N.G., 1999. The UIUC 3-D stratospheric chemical transport model: description and evaluation of the simulated source gases and ozone. Journal of Geophysical Research 104, 11755–11781.

Sebacher, D.I., Harriss, R.C., Bartlett, K.B., Sebacher, S.M., Grice, S.S., 1986. Atmospheric methane sources: Alaskan tundra bogs, an alpine fen, and sub-arctic boreal marsh. Tellus 38B, 1–10.

Simpson, I.J., Edwards, G.C., Thurtell, G.W., den Hartog, G., Neumann, H.H., Staebler, R.M., 1997. Micrometeorological measurement of methane and nitrous oxide exchange above a boreal aspen forest. Journal of Geophysical Research 102, 29331–29341.

Tohjima, Y., Wakita, H., Maksyutov, S., Machida, T., Inoue, G., Vinnichenko, N., Khattatov, V., 1997. Distribution of tropospheric methane over Siberia in July 1993. Journal of Geophysical Research 102 (D21), 25371–25382.

VNIIGAZ, 1998. Summarizing map of gas and oil deposits in the North of Tumen area. Gazprom, Moscow.

Whalen, S.C., Reeburgh, W.S., 1988. A methane flux time series for Tundra environments. Global Biogeochemical Cycles 2 (4), 399–409.

Worthy, D.E.J., Levin, I., Trivett, B.A., Kuhlmann, A.J., Hopper, J.F., Ernst, M.K., 1998. Seven years of continuous methane observations at a remote boreal site in Ontario, Canada. Journal of Geophysical Research 103, 15995–16007.

Zienkiewicz, O.C., 1971. The Finite Element Method in Engineering Science. McGraw-Hill, London, 368pp.

Zilitinkevich, S.S., 1970. Dynamics of Atmospheric Boundary Layer. Gydrometizdat, Leningrad, pp. 292 (in Russian).